Rice

RESEARCH Open Access

Spatio-Temporal Regulation of Gibberellin Biosynthesis Contributes to Optimal Rhizome Bud Development

Kanako Bessho-Uehara[1*], Tomoki Omori[2], Stefan Reuscher[2,3], Keisuke Nagai[2], Ayumi Agata[4], Mikiko Kojima[5], Yumiko Takebayashi[5], Takamasa Suzuki[6], Hitoshi Sakakibara[4,5], Motoyuki Ashikari[2] and Tokunori Hobo[2*]

Abstract

The perennial life cycle involves the reiterative development of sexual and asexual organs. Asexual structures such as rhizomes are found in various plant species, fostering extensive growth and competitive advantages. In the African wild rice *Oryza longistaminata*, we investigated the formation of rhizomes from axillary buds, which notably bend diagonally downward of the main stem, as the factors determining whether axillary buds become rhizomes or tillers are unclear. Our study revealed that rhizome buds initiate between the third and fifth nodes of seedlings beyond the 6-leaf stage, while the buds above the sixth node develop into tillers. We propose that precise regulation of gibberellin (GA) biosynthesis plays a pivotal role in optimal rhizome bud development, as demonstrated by a comparative transcriptome analysis between tiller buds and rhizome buds and quantification of phytohormones. Furthermore, GA_4 treatment upregulated the expression of genes associated with flowering repression and cell wall modification. These findings highlight the integration of GA biosynthesis and flowering repression genes as crucial in asexual organ development, shedding new light on the molecular mechanisms governing rhizome bud development in *O. longistaminata* and deepening our understanding of asexual reproduction regulation in perennial plants.

Keywords Rhizome, Axillary bud, Gibberellin, *Oryza longistaminata*, Reproductive strategy

Background

Angiosperms, encompassing approximately 300,000 species on Earth (Cronquist 1968), display a wide array of reproductive strategies. While sexual reproduction through flowers is the predominant mode for most angiosperms, many species employ vegetative reproduction, giving rise to various asexual reproductive organs such as tubers, bulbs, stolons, and rhizomes (Klimes et al. 1997). Most of the species that employ vegetative reproduction can also produce flowers, suggesting the existence of regulatory systems that maintain a balance between developing sexual organs (flowers) and asexual organs. Understanding the molecular mechanisms underlying

*Correspondence:
Kanako Bessho-Uehara
kanako.bessho.b3@tohoku.ac.jp
Tokunori Hobo
hobo.tokunori@gmail.com
[1]Graduate School of Life Sciences, Tohoku University, Sendai, Miyagi 980-8578, Japan
[2]Bioscience and Biotechnology Center, Nagoya University, Chikusa, Nagoya, Aichi 464-8601, Japan
[3]Present address: KWS SAAT SE & Co. KGaA, Grimsehlstr. 31. Postfach 1463, 37555 Einbeck, Germany
[4]Department of Applied Biosciences, Graduate School of Bioagricultural Sciences, Nagoya University, Chikusa, Nagoya, Aichi 464-8601, Japan
[5]RIKEN Center for Sustainable Resource Science, 1-7-22, Tsurumi, Yokohama, Kanagawa 230-0045, Japan
[6]College of Bioscience and Biotechnology, Chubu University, Matsumoto-cho, Aichi 487- 8501 Kasugai, Japan

the development of these asexual organs is vital for better understanding plant reproduction and evolution.

The molecular mechanisms underlying flower initiation have been extensively dissected (Simpson et al. 1999; Chanderbali et al. 2010; Romera-Branchat et al. 2014). *FLOWERING LOCUS T* (*FT*) is a key gene that initiates the transition of the shoot apical meristem (SAM) to a reproductive meristem that produces floral organs (Turck et al. 2008). The *CONSTANS–FT* module is at the core of the photoperiodic pathway in leaves that promotes flowering in response to daylength (Simpson et al. 1999). The transcription factor FD and 14-3-3 proteins interact with FT protein at the shoot apex to form the florigen activation complex (FAC) and promote the expression of *SUPPRESSOR OF OVEREXPRESSION OF CONSTANS1* (*SOC1*) and *APETALA1* (*AP1*), thus inducing the formation of floral meristems (Devlin and Kay 2000; Taoka et al. 2011; Teotia and Tang 2015). TERMINAL FLOWER 1 (TFL1), classified into same protein family of FT, interacts with 14-3-3 and FD to repress the expression of downstream flowering genes, conferring on TFL1 a function antagonistic to that of FT (Kaneko-Suzuki et al. 2018). These flowering-related genes and the underlying gene regulatory module are highly conserved across angiosperms (Bowman 1997; Chanderbali et al. 2010). By contrast, vegetative reproduction remains poorly understood, with the exception of tuber formation in potato (*Solanum tuberosum*). The *FT*-like gene *SELF-PRUNING 6 A* (*StSP6 A*) in potato encodes a major factor in tuber formation (Navarro et al. 2011) that forms the FAC with 14-3-3 and FD-like proteins (Hannapel et al. 2017). This result indicates that FT has several roles in inducing alterations of meristem identity, not only for the floral transition but also for tuber formation. In addition, *CENTRADIALIS* (*StCEN*), *TFL1* gene in potato, works as a repressor of tuber formation (Zhang et al. 2020).

Compared to our understanding of tuber formation, much less is known about the molecular mechanisms controlling rhizome development. A rhizome is also a type of asexual organ, consisting of an underground stem that elongates horizontally in the soil. Strong rhizomes contribute to the competitiveness and invasiveness of many grasses, which can sometimes be considered a harmful trait in crop fields (Jang et al. 2006; He et al. 2012). Rhizomes also play important roles in the establishment of the plant body and sustain plant growth, thus increasing biomass (Caruana et al. 2018). As plants from ferns to vascular plants produce rhizomes, understanding the molecular mechanisms of rhizome development would reveal how it evolved during plant diversification.

Cultivated rice (*Oryza sativa*) lacks a rhizome and reproduces sexually, via seeds (Fig. 1a). By contrast, the perennial African wild rice *Oryza longistaminata* reproduces mainly via rhizomes (Fig. 1b). The shape of the axillary bud that later gives rise to a rhizome (hereafter "rhizome bud") in *O. longistaminata* is different from that of a normal axillary bud ("tiller bud"): rhizome buds develop thick scale leaves and bend diagonally downward to take on an onion-like round shape (Yoshida et al. 2016). After completing the development of this specific bud shape, rhizome internodes start to elongate under the soil. The rhizome then grows upwards and reaches the soil surface, above which is becomes an aerial shoot. Based on observations of underground organs (Bessho-Uehara et al. 2018), rhizome development can be classified into three steps: (1) rhizome bud formation, (2) internode elongation, and (3) emergence of the rhizome tip above the soil surface (Fig. 1c). The axillary buds located on each node of the rhizome contribute to vegetative reproduction by undergoing this developmental stage repeatedly, thereby supporting vegetative reproduction. Although rhizome growth was shown to be regulated by light (Fan et al. 2017), temperature (Wang et al. 2024), and several phytohormones (Hu et al. 2011; Shibasaki et al. 2021; Kawai et al. 2022), the molecular mechanisms underlying rhizome bud development, especially at the initial step, had not been elucidated.

Here, we determined the exact stage of rhizome bud initiation in *O. longistaminata* and demonstrate that spatio-temporal GA_4 accumulation is important for optimal rhizome bud initiation by performing physiological experiments and a comparative transcriptome analysis. Transcriptome analysis suggested that GA_4 and *TFL1* might contribute to maintaining the meristem of rhizome buds in a vegetative state. This work highlights how the fine-tuned expression pattern of GA biosynthesis genes is essential for optimal GA_4 accumulation, which influences the fate transition from an axillary bud to a rhizome bud in *O. longistaminata*.

Results

Determination of Initial Timing of Angle Alteration in Rhizome Buds

The rhizome bud grows diagonally and downward from the main stem while a tiller bud grows upward and parallel to the parental stem (Yoshida et al. 2016). To determine when the alteration in bud angle first takes place, we inspected longitudinal sections of rhizome buds at several growth stages. Axillary buds at the third node were collected from *O. sativa* and *O. longistaminata* plants grown from seed at the 5-, 6-, and 7-leaf stage for sectioning (Fig. 1d, Fig. S1a, b). In *O. sativa*, the axillary bud at the third node consistently grew upward at all examined leaf stages (Fig. 1e–g), unlike in *O. longistaminata* where the direction changed after the 6-leaf stage (Fig. 1h–j). When we allowed *O. longistaminata* seedlings to grow until the 9-leaf stage, the axillary bud exhibited a change in its angle and started to develop into a

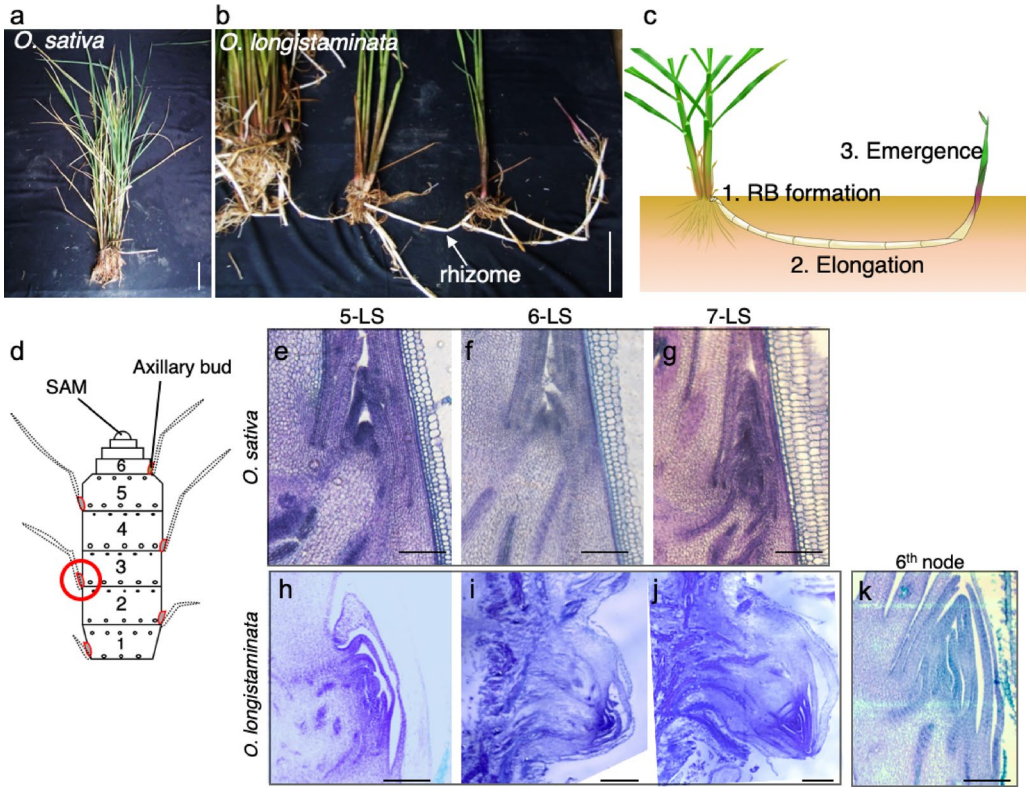

Fig. 1 Morphological differences between the axillary buds of *O. sativa* and *O. longistaminata*. (a) Cultivated rice (*Oryza sativa*) propagates by seeds and does not form rhizomes. (b) The African wild rice *O. longistaminata* propagates by rhizomes. Some roots were removed prior to taking the photograph to facilitate rhizome observation. Scale bars in (a, b), 10 cm. (c) Diagram of the three steps of rhizome development in *O. longistaminata*. RB, rhizome bud. (d) Diagram of a rice seedling. The numbers indicate internodes. The red circle indicates the axillary buds observed in this study. SAM, shoot apical meristem. (e–j) Longitudinal sections of the axillary bud at the third node from *O. sativa* (e–g) and *O. longistaminata* (h–j) at the 5-, 6-, and 7-leaf stages. (k) Longitudinal section of the axillary bud at the sixth node at the 7-leaf stage in *O. longistaminata*. Scale bars in (e–k), 1 mm

long rhizome (Fig. S1**c**). The axillary buds from the sixth node at the 7-leaf stage grew upward as tiller buds in *O. longistaminata* (Fig. 1k), as did all of the axillary buds above the sixth node. These results suggest that the angle alteration of axillary buds starts from the 6-leaf stage at the third node, leading to the formation of a rhizome bud.

Rhizome Growth in Cuttings and Plants Grown from Seed is Comparable

To efficiently study rhizome bud development, we established a cutting-based propagation system for *O. longistaminata*, which rarely produces fertile seeds due to heavily relying on vegetative reproduction. In this system, aerial stems with a single axillary bud were cut and planted with the node buried (Fig. S2a–c), allowing the axillary bud to grow into a primary tiller within a week (Fig. S2d). Rhizome formation from secondary axillary buds occurred four weeks after cutting (Fig. S2e). As in seedlings, rhizomes appeared from the 8-leaf stage and developed into aerial shoots by the 13-leaf stage (Fig. 2a–c).

To characterize rhizome bud morphology, we examined longitudinal sections of secondary axillary buds from the third node of cuttings at the 5-, 6-, and 7-leaf stages. Secondary axillary buds of *O. longistaminata* cuttings grew upward and parallel to the primary tiller until the 5-leaf stage (Fig. 2d), but altered their growth angle downward and against the primary tiller at the 6-leaf stage, eventually penetrating the leaf sheath of the primary tiller and growing horizontally at the 7-leaf stage (Fig. 2e, f). Secondary axillary buds thus became rhizome buds starting at the 6-leaf stage. We also measured the angle formed between the secondary axillary bud and the primary tiller from the first to the seventh node at the 6- and 8-leaf stages of cuttings (Fig. 2g). Axillary bud angle alteration began at the third node from the 6-leaf stage (Fig. 2h). At this stage, buds at the fourth node also showed a marked change in angle, averaging over 80° relative to the primary tiller. By the 8-leaf stage, axillary buds at the fifth node likewise altered their angle (Fig. 2h). In parallel, secondary buds began elongating into rhizomes from the fourth and fifth nodes specifically at the 8-leaf stage, a change not apparent at the 6-leaf stage (Fig. 2i). These observations indicate that cuttings form rhizome buds from secondary axillary buds at the 6-leaf stage, primarily

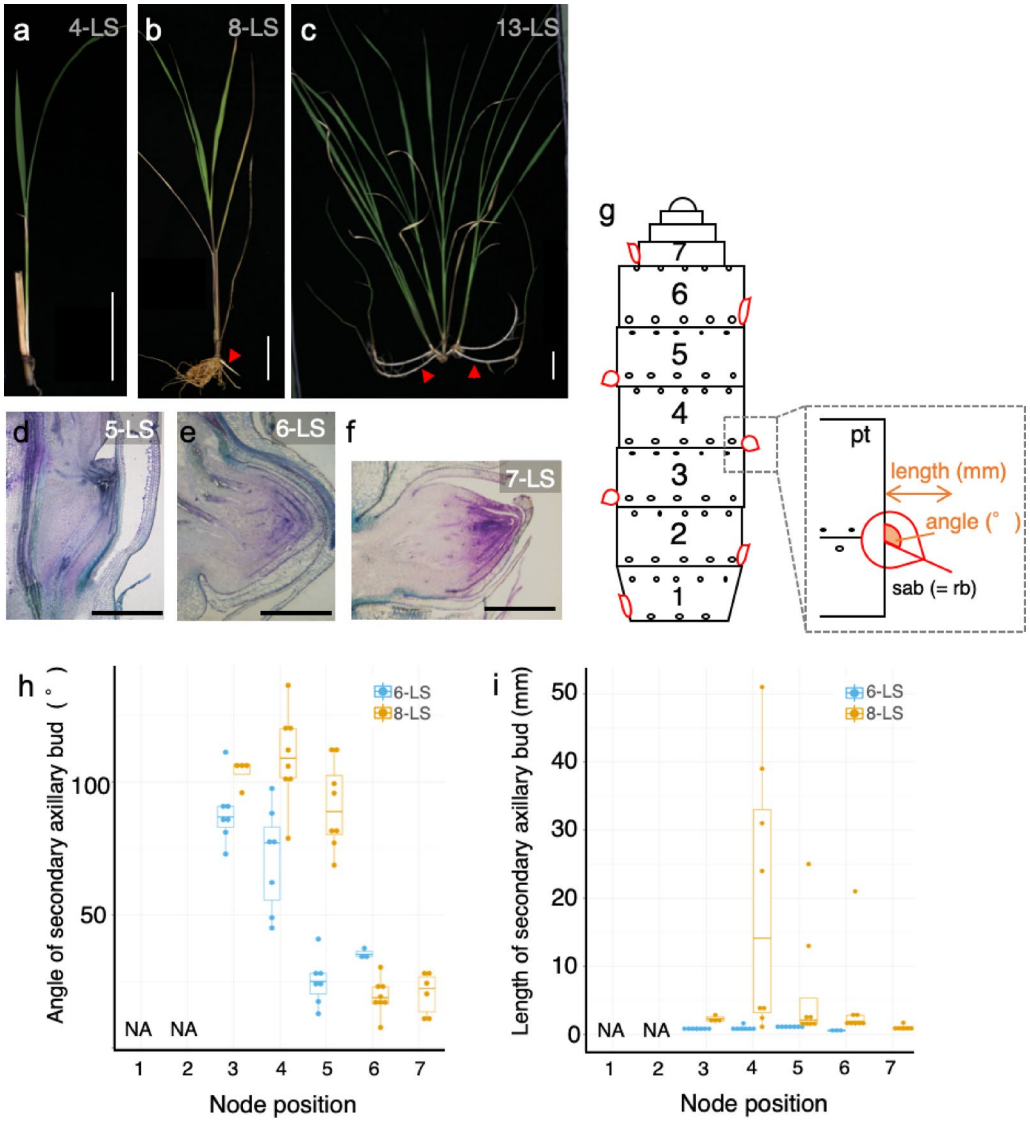

Fig. 2 Rhizome morphology derived from cuttings. (a–c) Cuttings of *O. longistaminata* at the 4-leaf stage (a), 8-leaf stage (b), and 13-leaf stage (c). The red arrowheads indicate rhizomes growing from secondary axillary buds. (d–f) Longitudinal sections of the primary tiller from the third node at the 5- (d), 6- (e), and 7-leaf stage (f). Scale bars, 5 mm. (g) Diagram of rice seedling showing the method of angle measurement for the secondary axillary bud. Pt, primary tiller derived from cutting; sab, secondary axillary bud from primary tiller; rb, rhizome bud. Details are provided in **Methods**. (h, i) Angle (h) and length (i) of the secondary axillary bud against the abaxial side of the primary tiller at the 6- or 8-leaf stage. The *x*-axis indicates the node position. Each dot represents an individual seedling. NA = not applicable. LS, leaf stage.

at the third to fifth nodes, consistent with the pattern in seedlings grown from seed.

The Transcriptomes of Tiller and Rhizome Buds from Cuttings are Significantly Different

To investigate the dynamics of gene expression in axillary buds, we performed a transcriptome analysis using axillary buds collected from the third node (before and after bending) and the seventh node (tiller bud) of cuttings (Fig. 3a). Principal component analysis (PCA) indicated that tiller buds and rhizome buds are clearly separated by the PC1, while rhizome buds before and after bending were distinguished by PC2 (Fig. 3b). The number of differentially expressed genes (DEGs) in pairwise comparisons also highlighted the differences between tillers and rhizome buds before or after bending, with fewer DEGs detected between the two types of rhizome buds (Fig. S3a, Table S1). A gene ontology (GO) enrichment analysis revealed an upregulation of genes involved in light-harvesting system and carbon fixation in tiller buds relative to rhizome buds, suggesting that these axillary buds are preparing for photosynthesis at this stage, although they have not been exposed to light (Cluster A, Fig. 3c, Fig. S3b, Table S2). Moreover, the expression

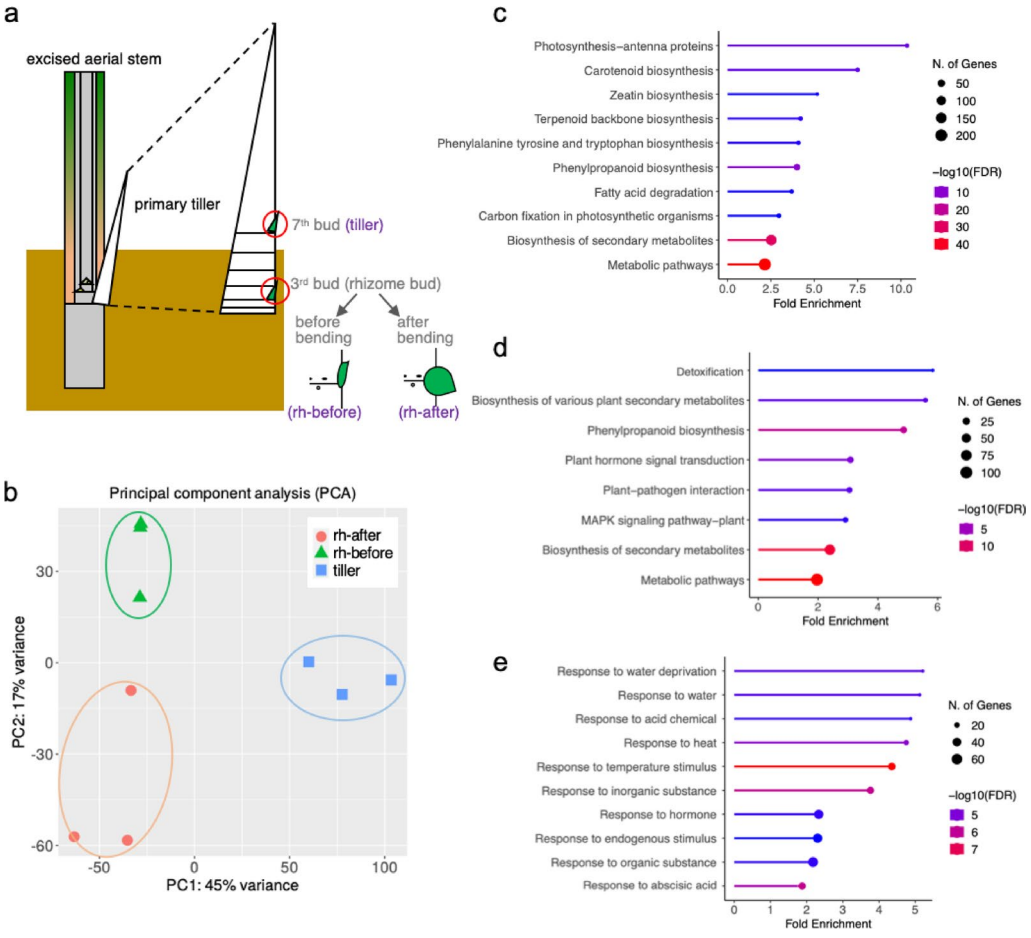

Fig. 3 Transcriptome analysis of cuttings of *O. longistaminata*. (a) Diagram of the collected samples. Axillary buds at the seventh node (indicated as 7th bud) were collected as tiller buds. Axillary buds at the third node (indicated as 3rd bud) were collected as rhizome buds and divided into before-bending and after-bending rhizomes (indicated as rh-before and rh-after in the figure, respectively). (b) Principal component analysis (PCA) of all transcripts from the three replicates for tillers and rhizome buds before or after bending. (c-e) Gene ontology (GO) terms enriched in each cluster. Cluster A (upregulated in tiller bud) (c), B (upregulated in both before- and after-bending rhizome bud) (d), and C (upregulated in after-bending rhizome bud) (e) respectively indicated in Fig. S3b.

of genes related to "Detoxification" and "Plant-pathogen interaction" was significantly upregulated in rhizome buds before and after bending (Cluster B, Fig. 3d, Table S2). The expression of genes responding to abiotic factors such as temperature, osmotic pressure, and inorganic/organic substances, as well as a group of abscisic acid (ABA)-responsive genes, was specifically elevated in developed rhizome buds after bending (Cluster C, Fig. 3e, Table S2). These results likely reflect the adaptation to the above- and under-ground environments, and also suggest that rhizome buds after bending have acquired tolerance to various stresses.

GA Accumulation is Different Between Tiller and Rhizome Buds

Phytohormones have fundamental roles in plant growth and development (Kepinski 2006). To determine which phytohormones regulate rhizome bud development in *O. longistaminata*, we measured the levels of several phytohormones and their precursors in several tissues (Table S3). Based on axillary buds morphology, we collected the tip parts of mature rhizomes (5 cm < length < 10 cm) containing buds before bending, and middle parts containing buds after bending (Fig. 4a). We also collected immature rhizomes (length < 5 cm), SAM regions of the aerial shoot at the vegetative stage of *O. longistaminata* and *O. sativa*, and SAM regions of the reproductive stage of *O. sativa* stem for comparison.

To classify each type of tissue based on their phytohormone contents, PCA was performed (Fig. 4b). We observed a separation of samples by species along PC1, which explained 24% of the total variance, while PC2 sorted *O. sativa* samples based on their vegetative or reproductive status. The *O. longistaminata* samples showed a more complex pattern. The middle part of mature rhizomes with developed rhizome buds was

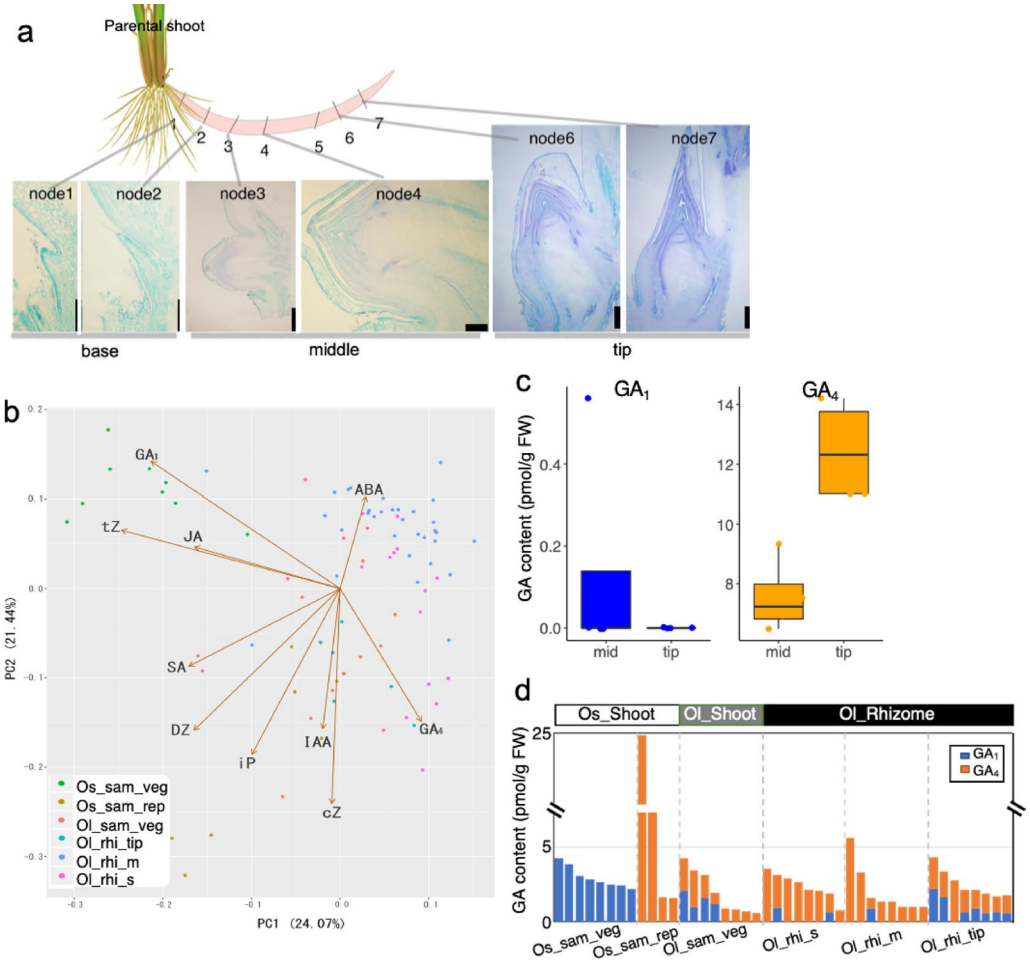

Fig. 4 Effects of phytohormones on rhizome development. (a) Morphology of axillary buds at each node of a mature rhizome. (b) Principal component analysis (PCA) of all detected phytohormones in various organs of *O. sativa* (Os) and *O. longistaminata* (Ol). Os_sam_veg, *O. sativa* shoot in the vegetative stage; Os_sam_rep, *O. sativa* shoot in the reproductive stage; Ol_sam_veg, *O. longistaminata* shoot in the vegetative stage; Ol_rhi_tip, rhizome tip including axillary bud before bending; Ol_rhi_m, middle of rhizome including axillary bud after bending; Ol_rhi_s, short rhizome (length < 5 cm) including axillary bud before bending. (c) Contents of the active GAs GA_1 and GA_4 at the rhizome tip (tip) and middle part (mid) of mature rhizomes. (d) Contents of active GAs in *O. sativa* and *O. longistaminata* at each node of a mature rhizome. Sample labels are as in (b).

distinct from other *O. longistaminata* tissues in terms of their phytohormone contents. By contrast, immature rhizomes were distributed over the entire dimension defined by PC2, possibly reflecting the varied phytohormone contents of these tissues, which included several stages of rhizome buds before and after bending. The phytohormone contents in the tips of mature rhizomes and some immature rhizomes displayed the same pattern as those from the aerial shoots of *O. longistaminata*, suggesting that these samples with axillary buds resembling tiller buds in their morphology have the same plant hormone characteristics as aerial tissues. Principal component loadings indicated that the two phytohormones ABA and gibberellic acid (GA_4) appear to be associated with the distinct clustering of *O. longistaminata* samples relative to *O. sativa* (Fig. 4b). In addition, we detected GA_1 rarely in rhizomes, but GA_4 accumulated to higher levels in rhizome tips, which carry rhizome buds before bending, than in the middle of rhizomes, which contain rhizome buds after bending (Fig. 4c). Notably, the accumulation pattern of GAs contributed to the separation of samples by genotype: GA_1 accumulation was associated with *O. sativa* vegetative SAMs, while GA_4 accumulated in *O. sativa* reproductive SAMs and *O. longistaminata* tissues (Fig. 4d). These results indicate that GA_4 and ABA might responsible for the development of rhizome buds before and after bending, respectively.

High *GA20ox2* Transcript Levels and High GA20ox2 Enzymatic Activity Contribute to the Spatio-Temporal GA_4 Accumulation Pattern in Rhizome Buds

To clarify the difference of GA amount between rhizome buds before and after bending, we manually checked GA biosynthesis genes specifically expressed in rhizome

buds. The expression level of *GA20 oxidase 2* (*GA20ox2*) is higher in rhizome buds before bending than in the other two types of buds (Fig. 5a). There were no significant differences in the expression levels of other *GA20ox* genes among these three types of buds, with overall low expression levels. Among other GA biosynthesis genes (Fig. S4a, Table S4), several genes showed tissue-specific expression. For instance, *ent-KAURENOIC ACID HYDROXYLASE* (*KAO*), encoding the enzyme converting the precursor *ent*-kaurenoic acid to GA_{12} upstream of the GA_1 and GA_4 pathways, was more highly expressed in rhizome buds regardless of developmental stage (Fig. S4b). The expression pattern of *GA13ox1* converts GA_{12} to GA_{53}, was barely expressed across all samples, whereas *GA13ox2* showed a similar pattern as *KAO* (Fig. S4c, d). *GA3ox* genes encoding the enzyme that catalyzes the final step in the production of active GAs were also largely not expressed (*GA3ox1*) or had slightly higher expression in rhizome buds than in tiller buds (*GA3ox2*) (Fig. S4e, f).

The expression pattern of *GA20ox2* in *O. longistaminata* rhizome buds collected from cuttings at the 5- and 6-leaf stages was examined by *in situ* hybridization. We detected a strong signal for *GA20ox2* transcripts in axillary buds at the 5-leaf stage, especially at the leaf axils and the tip of leaf primordia (Fig. 5b). By contrast, the signal strength for *GA20ox2* transcripts greatly diminished at the 6-leaf stage when the axillary bud had completely bent downward (Fig. 5c). These results suggest that the expression levels of *GA20ox2* rise before axillary buds alter their growth angle (~ 5-leaf stage) and decrease after the completion of rhizome bud formation.

Phytohormone concentrations reflect the transcriptional and post-transcriptional regulation of the genes encoding their biosynthetic enzymes, as well as the activity of these enzymes. The deepwater rice cultivar 'C9285' (*O. sativa* ssp. *indica*) was previously shown to have a highly active form of GA20ox2 (Kuroha et al. 2018), due to two amino acid substitutions (E100G and Q340R, abbreviated GR) relative to GA20ox2 of *O. sativa* ssp. *japonica* cultivar 'T65' (abbreviated EQ). Indeed, $GA20ox2^{GR}$ catalyzes GA precursors within the GA_4 pathway faster than $GA20ox2^{EQ}$ (Kuroha et al. 2018). We determined that the *O. longistaminata* genome encodes a GR-type GA20ox2 enzyme, with an additional six amino acids in the C-terminal region relative to that of *O. sativa* (Fig. 5d, Fig. S5). Together, these results suggest that the combination of higher *GA20ox2* transcript levels in rhizome buds before bending and the high predicted enzymatic activity of GA20ox2 of *O. longistaminata* promotes GA_4 biosynthesis in rhizomes.

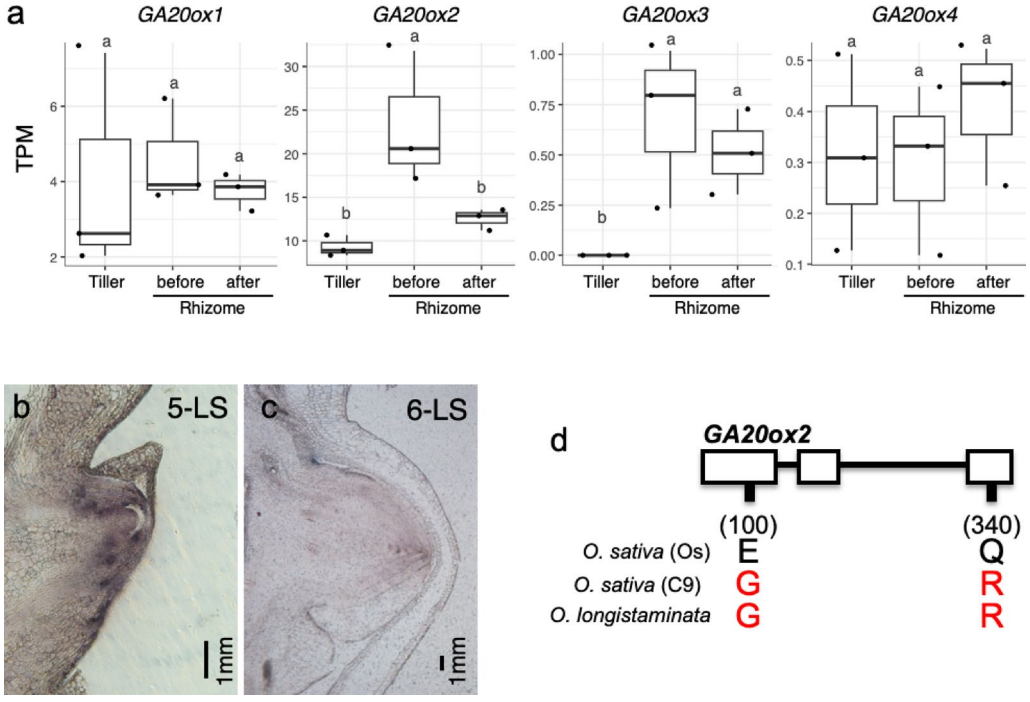

Fig. 5 Expression pattern of GA biosynthesis genes at the rhizome bud. (a) Expression levels of the *GA20ox* genes in tiller and rhizome buds of cuttings, shown as transcripts per million (TPM) values from RNA-seq data. Different lowercase letters indicate significant differences, as determined by one-way analysis of variance (ANOVA) followed by Tukey's multiple-comparison test. (b, c) RNA *in situ* hybridization of *GA20ox2* transcripts at the axillary bud of the fourth node at the 5-leaf stage (b) or the 6-leaf stage (c) of cuttings of *O. longistaminata*. (d) Diagram of the *GA20ox2* locus and amino acid substitutions of its encoding protein in *O. sativa* (Os), deepwater rice (C9), and *O. longistaminata*. White boxes indicate exons. Red letters indicate amino acid substitutions specific to C9 and O. longistaminata.

Effects of Manipulating GA Signaling Output on the Angle Alteration of Rhizome Buds

To examine the effects of GA_4 on axillary bud development, we treated *O. longistaminata* cuttings from the 5-leaf stage with GA_4 and/or the GA biosynthesis inhibitor uniconazole (UNI). In mock-treated cuttings, axillary buds at the fourth node developed into rhizomes (Fig. 6a). UNI treatment (10^{-5} M) altered this growth, producing upward-growing tiller-like buds (Fig. 6b). To examine whether GA content influenced this effect, we applied three different concentrations of GA_4 (10^{-7} M, 10^{-6} M, or 10^{-5} M) to UNI-treated cuttings. Lower and moderate GA_4 concentrations (10^{-7} M and 10^{-6} M) rescued the effects imposed by UNI treatment and returned the angle of axillary buds as observed in mock-treated cuttings (Fig. 6a, c, d, f). However, the highest concentration (10^{-5} M) of GA_4 prevented downward growth, maintaining upward bud growth (Fig. 6e, f). An increasing GA_4 concentration applied to UNI-treated cuttings was also accompanied by less rhizome elongation, from about 40 mm in mock-treated cuttings to 15 mm when treated with 10^{-5} M UNI + 10^{-7} M GA_4 (Fig. S6). Higher GA_4 concentrations of 10^{-6} M or 10^{-5} M resulted in even shorter rhizomes, while overall plant height increased, as expected for GA-treated plants. This may reflect a trade-off in resource allocation between above- and underground. These results suggest that GA_4 contribute to regulate the axillary bud bending. Together with the decline in *GA20ox2* expression upon the completion of rhizome bud formation, we propose that spatio-temporal regulation of GA levels is important for proper rhizome bud development.

Transcriptome Changes of the Axillary Bud Response to GA Treatment Between *O. sativa* and *O. longistaminata*

To understand how GA_4 affects axillary bud gene expression, we analyzed transcriptomes from the axillary buds of *O. sativa* (Os) and *O. longistaminata* (Ol) cuttings treated with GA and UNI, or mock solvent (Fig. S7). A low Pearson's correlation (– 0.09) between differentially expressed genes (DEGs) in the two species suggested distinct responses to UNI treatment (Fig. 7a). Gene ontology (GO) enrichment analysis showed that in *O. sativa*, "photosynthesis" (GO: 0015979) and "response to light stimuli" (GO: 0009416, GO: 0009644, and GO: 0009645) related genes were upregulated (Fig. S8, Table S5). This result suggested that *O. sativa* axillary buds prepare for light exposure before becoming exposed to light, as did tiller buds of *O. longistaminata* (Fig. 3c). In contrast, *O. longistaminata* samples were enriched the GO terms related to catabolizing cell wall components (GO:0000272, GO:0006032, and GO:0016998) and killing cells of other organisms (GO:0031640) —traits relevant to underground growth (Fig. S8, Table S5).

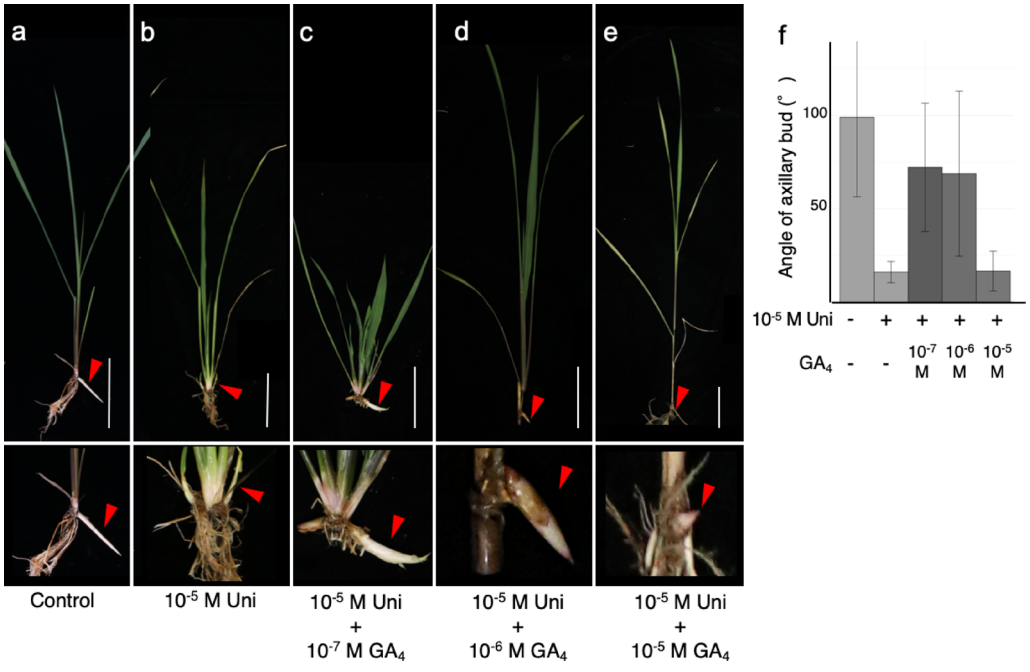

Fig. 6 Effect of GA signaling on the angle of rhizome buds. (a–e) Cuttings of *O. longistaminata* observed at the 6-leaf stage mock-treated with solvent only (a) or treated with 10^{-5} M of the GA biosynthetic inhibitor uniconazole (UNI) alone (b) or together with 10^{-7} M (c), 10^{-6} M (d), or 10^{-5} M (e) GA_4. Three samples are used with each treatment. Upper panels show entire plants; lower panels are magnified views of the buds at the fourth node, indicated by the red arrowheads. Scale bars (upper panels), 10 cm. (f) Angle of secondary axillary buds (measured from the primary tiller) at the fourth node across treatments. Data are shown as means ± standard deviation (SD).

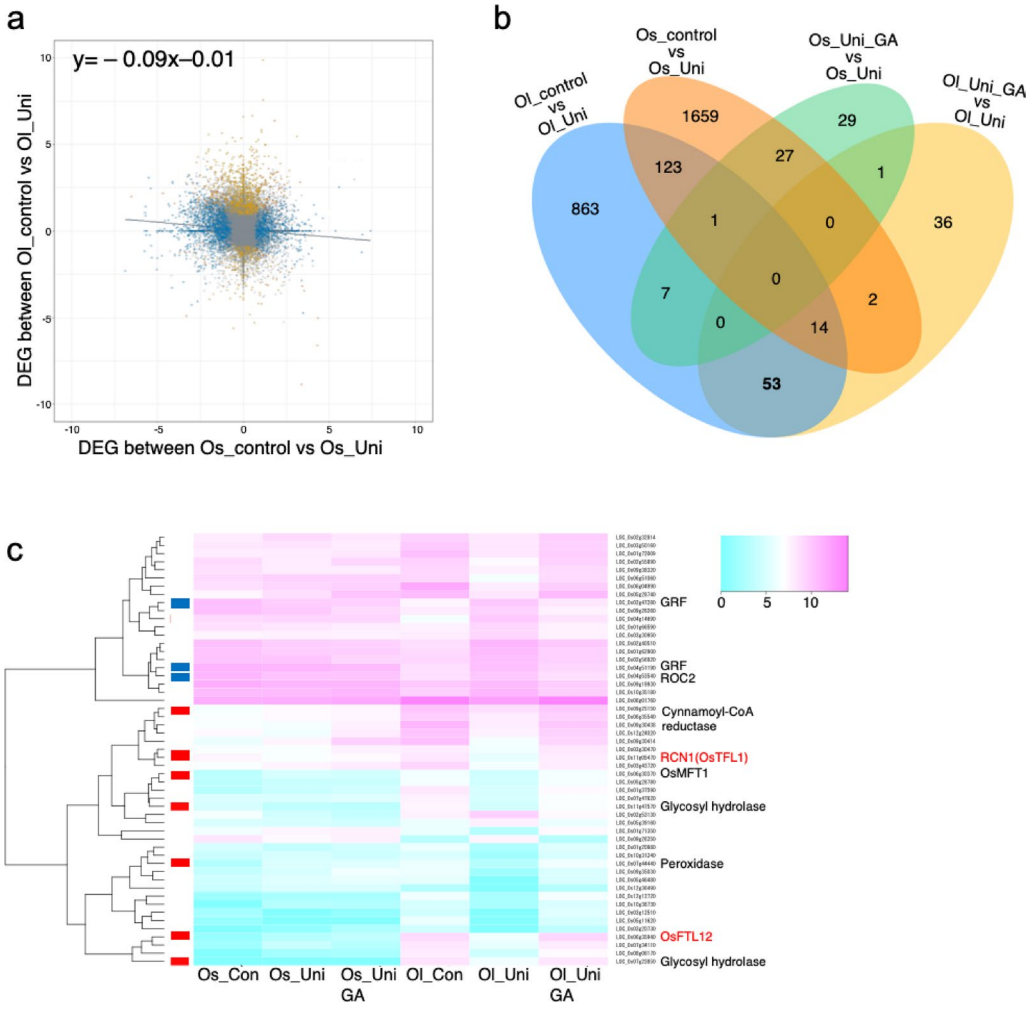

Fig. 7 Transcriptome analysis of the effects of GA treatment on rhizome bud initiation. (a) Scatterplot of differentially expressed genes (DEGs) in *O. sativa* and *O. longistaminata* cutting samples upon uniconazole (UNI) treatment. The *y*-axis shows the $\log_2$ ratio of expression for DEGs between mock-treated and UNI-treated *O. longistaminata* cuttings (orange dots); the *x*-axis shows the $\log_2$ ratio of expression for DEGs between mock-treated and UNI-treated *O. sativa* cuttings (blue dots). The solid line represents the regression line. Gray dots represent genes with comparable expression levels between mock-treated and UNI-treated cuttings. (b) Venn diagram showing the extent of overlap between DEGs across the indicated pairwise comparisons. (c) Heatmap representation of the expression of 53 genes commonly expressed in *O. longistaminata* following treatment with mock and GA_4. The red and blue squares to the left of the heatmap indicate highly expressed genes in *O. longistaminata* treated with GA_4 or UNI, respectively. The color scale indicates $\log_2$ fold-change.

Ethylene-mediated signaling (GO: 0009871) was also specifically enriched in *O. longistaminata* samples treated with GA_4 (Table S5). These results suggest that *O. sativa* and *O. longistaminata* employ different transcriptional responses to GA pathway manipulation. A Venn diagram of DEGs revealed only 138 genes shared between the two species, underscoring their divergent regulatory mechanisms (Fig. 7b, Table S6), representing 7% (*O. sativa*) and 13% (*O. longistaminata*) of all DEGs in each sample. We conclude that *O. sativa* and *O. longistaminata* follow different gene expression programs in response to exogenous treatment with GA_4 or UNI.

GA_4 Upregulates the Expression of Negative Regulator of Flowering and Chitinase Family Genes Specifically in *O. longistaminata*

From the Venn diagram, we identified 53 genes that are differentially expressed specifically in *O. longistaminata* (Fig. 7b). We performed a clustering analysis of these 53 genes to compare their expression patterns in *O. sativa* and *O. longistaminata*. Notably, the expression profile of these 53 genes was similar in *O. sativa* and in UNI-treated *O. longistaminata* buds, both of which exhibit upward bud growth (Fig. 7c, Table S7). In contrast, mock- and GA_4-treated *O. longistaminata* samples, which form normal rhizomes, showed elevated expression of flowering repressors such as *FT-like12* (*OsFTL12*,

LOC_Os06 g35940), and *Rice CENTRORADIALIS-like 1* (*RCN1*, LOC_Os11 g05470) that is a homolog of *TFL1*. *OsFTL12* and *RCN1* are known to repress floral transition in rice and may help maintain rhizome buds in a vegetative state.

We also detected several chitinase genes (LOC_Os03 g30470, LOC_Os07 g23850, LOC_Os11 g47570) as being highly expressed in mock-treated and GA_4-treated samples from *O. longistaminata*, but not in UNI-treated samples or in *O. sativa*. We hypothesize that rhizomes need to respond to several biotic and abiotic stresses, especially to microorganisms in the soil.

Treatment with a GA Biosynthesis Inhibitor Induces the Expression of Transcription Factor Genes in *O. longistaminata*

UNI-treated *O. longistaminata* and *O. sativa* cuttings showed elevated expression of several transcription factor genes, including growth-regulating factor (GRF) homologs, LOC_Os02 g47280 and LOC_Os04 g51190 (Fig. 7c, Table S7). OsGRFs bind to the promoter region of the *Knotted1-like homeobox* (*KNOX*) gene, which encodes a central regulator of SAM development, and thus repress *KNOX* expression (Kuijt et al. 2014). The GRF–*KNOX* regulatory module might contribute to the development of axillary bud meristems, whereby GA_4 inhibits *GRF* expression and thus promotes the development of an axillary bud into a rhizome bud. These results suggest that UNI treatment represses the expression of transcription factor genes that may affect rhizome development, thus preventing diagonal downward growth and promoting upward growth instead.

Discussion

Rhizome-mediated vegetative propagation is widespread across land plants, from ferns to angiosperms, suggesting that its molecular mechanisms may be broadly conserved. However, as angiosperms have evolved to develop flowers, they may have acquired the mechanisms to balance vegetative reproduction with sexual (seed) reproduction within individuals. Understanding how plants orchestrate this balance is important for revealing the diversification of reproductive strategies in angiosperms.

In this study, we identified the timing and location at which axillary buds begin to develop into rhizome buds by examining both seedlings and cuttings of *O. longistaminata*. Our transcriptome analysis showed that GA plays a key role in rhizome buds before bending, while ABA becomes prominent afterward and it was consistent with the PCA loading by hormone quantification (Fig. 4b). This pattern aligns with single cell RNA-seq results indicating GA downregulation and ABA upregulation in developed rhizome buds (Lian et al. 2024). *GA20ox2* expression pattern and its amino acid sequence further explain the temporal regulation of GA_4 during rhizome bud development. Treatment with GA_4 or the GA biosynthesis inhibitor UNI affected axillary bud angles, supporting GA's functional role in rhizome development. It should be noted that GA_4-treated aerial shoots developed longer, yellowing leaves compared to controls, possibly reflecting reduced photosynthetic output and thereby indirectly affecting bud morphology. However, single UNI treatment or UNI combined with 10^{-6} M GA_4 showed minimal differences from controls in plant height and leaf color, suggesting that GA_4 likely contributes directly or indirectly to bud angle alteration.

Exogenous GA_4 application provided further insight into GA's role at the molecular level. GA_4 treatment triggered widespread transcriptomic changes, altering the expression of genes related to ethylene signaling, cell wall metabolism, flowering repression, and transcription factors. Many of these GA-responsive genes likely prepare the bud for underground growth. For instance, upregulation of cell wall remodeling genes may reinforce rhizome tissues for underground penetration (Toriba et al. 2020), and early activation of defense-related genes may help prepare rhizome buds for soil microbes (He et al. 2014). In addition, GA_4 treatment resulted in increased expression of flower repressor genes such as *OsFTL12* and *TFL1*. *OsFTL12* belongs to the rice FT family and was recently reported to work as a flowering repressor (Zheng et al. 2023). Notably, the relationship between GAs and *TFL1* has been established in potato and strawberry. GAs have been reported to promote stolon formation in potato and strawberry (Kloosterman et al. 2007; Caruana et al. 2018). *TFL1* overexpression in potato led to a repression of tuber formation (Zhang et al. 2020) and a strawberry *tfl1* mutant produced flowers instead of stolons (Tenreira et al. 2017). Although direct genetic confirmation in *O. longistaminata* is currently impractical due to transformation difficulties, our results strongly implicate a similar GA–TFL1 regulatory module operating in rhizome bud development. These parallels suggest that rhizomes and stolons—two types of asexual organs that arose independently during angiosperm evolution—share a convergent molecular mechanism controlled in part by GA signaling and floral repressors.

In addition to hormonal control, small RNAs also contribute to maintaining rhizome buds in a vegetative state. Despite flowering in aerial shoots, rhizome tips in *O. longistaminata* remain vegetative (Yoshida et al. 2016). This may be maintained by high levels of microRNA156 (miR156), which suppress *SQUAMOSA PROMOTER BINDING PROTEIN-LIKE* (*SPL*) transcripts that promote flowering (Toriba et al. 2019). A similar involvement of miRNAs in the switch between reproductive and vegetative phase in individual plants was also observed in other perennial plant species, *Cardamine flexuosa*

(Bergonzi et al. 2013; Zhou et al. 2013). A common theme thus emerges that GAs promote vegetative growth in perennials at the expense of reproductive development. The integration of GA, miRNAs, and the floral repressor illustrates a regulatory mechanism for the production of asexual organs that may have contributed to the diversification of reproductive strategies in angiosperms.

The findings of this study suggest that the transition between the development of tiller buds which contribute to seed reproduction, and of rhizome buds which contribute to vegetative reproduction, is initiated by GA (Fig. S9). This might be the one of the mechanism to balance vegetative and sexual (seed) reproduction within individuals. Comparative analyses involving other vegetative propagating or perennial plant species should help uncover the complete picture of the signaling pathways underlying rhizome development.

Conclusion

We investigated the molecular mechanisms that drive rhizome bud development in *Oryza longistaminata*. This study underscores the critical role of gibberellin, especially GA_4, in regulating the development of axillary buds into rhizomes or tillers, contingent on their spatio-temporal accumulation patterns. Our findings from comparative transcriptome and phytohormone analysis suggest differential expression of genes related to gibberellin biosynthesis, delineating the unique growth directions and morphology distinguishing rhizome buds from tiller buds. This research provides insights into the phytohormonal and molecular mechanisms of asexual reproduction in plants through rhizome formation, with potential implications for agricultural practices and plant adaptability.

Methods

Plant Materials and Growth Conditions

Seeds of *O. longistaminata* (accession IRGC110404) were obtained from the International Rice Research Institute (IRRI), Philippines; seeds of *O. sativa* cultivars 'Nipponbare' and 'Taichung 65' (T65) were from the Ashikari lab seed stocks at Nagoya University, Japan. All plant materials were grown in a greenhouse under a 14-h light/10-h dark photoperiod, with an average temperature of 27 °C under natural sunlight and supplemented with metal halide lamps (MT360 CELS-W/BH, IWASAKI ELECTRIC, Tokyo) for 3 h in the evening until the 9-leaf stage. After the 9-leaf stage, the seedlings were transferred to a short-day photoperiod of 10-h light/14-h dark, with an average temperature of 27 °C. Plants were grown in Mikawa-baido soil (AICHI-MEDEL, Aichi).

Histological Analysis

The basal parts of Nipponbare and IRGC110404 seedlings grown from seeds until the 5-, 6-, and 7-leaf stages were collected for the longitudinal sections shown in Fig. 1. The basal parts of cuttings from *O. longistaminata* at the 5-, 6-, and 7-leaf stages were collected for the longitudinal sections shown in Fig. 2. Samples were fixed in FAA (5% [w/v] formaldehyde, 5% [v/v] acetic acid, 45% [v/v] ethanol, and 45% [v/v] water) overnight at 4 °C and dehydrated in a graded ethanol and butanol series before embedding in Paraplast plus (McCormick, MD, USA). Longitudinal sections of 10 μm in thickness were generated with a microtome (Leica RM2125RT) and placed onto glass slides (Matsunami Glass Ind. Ltd., Japan). Glass slides were heated to 50 °C on a hot plate (FinePlateHP40). After removing the Paraplast and adhering the sections onto the glass slides, the sections were rehydrated with a reverse graded ethanol series (100%, 90%, 75%, and 30% ethanol, all v/v in water) and with distilled water (dH_2O). The sections were then stained with 0.1% (w/v) toluidine blue. The stained sections were then dehydrated in a graded ethanol series, with the final step in 100% ethanol replaced with xylene and mounted in Eukitt® (Sigma-Aldrich, St. Louis, MO, USA). Stained sections were observed under a stereomicroscope (Leica, Wetzlar, Germany).

Inducing New Rhizome Buds by Cuttings of Aerial Shoots

Aerial shoots with elongated internodes from IRGC110404 and Nipponbare plants were cut such that each segment included one node. The node was then covered by soil in a plastic box (56 cm × 54 cm × 15 cm). Each box was filled with Mikawa-baido soil (AICHI-MEDEL, Japan) and contained four individual plants. The growth conditions were set to a 14-h light/10-h dark photoperiod with a temperature cycle of 27 °C/25 °C (day/night) in a Biotron (Nihon-ika, Japan). The cuttings were dug out from the soil to evaluate bud morphology at the indicated times or stages. Photographs of the cutting protocol are shown in Fig. S2.

Phenotypic Analysis

Grown secondary axillary buds were photographed from the first to the seventh nodes of IRGC110404 cuttings at the 6- or 8-leaf stage. In the photographs, the tip of the axillary bud was connected to the primary tiller by a line, and the angle on the axillary bud was measured using ImageJ (1.50e or later version) as shown in Fig. 2g. The length of axillary buds was measured with ImageJ. Boxplots representing the results were plotted using R (V3.3.2 or later version).

Transcriptome Analysis Using Cuttings of *O. longistaminata*

For each tissue type (tiller, rhizome bud before bending, rhizome bud after bending), three to eight axillary buds located at the third node (for rhizome buds) or seventh node (for tillers) of cuttings from IRGC110404 plants were collected in one tube and used as one replicate. Three replicates were prepared for each tissue type. Immediately after harvest, the samples were flash-frozen in liquid nitrogen and crushed with iron beads. Total RNA was extracted from each replicate using RNeasy Plant Kit (QIAGEN) following the manufacturer's instructions. RNA quality was measured on a Bioanalyzer, with only those samples with an RNA integrity number over 7 being used for the following steps. Sequencing libraries were constructed using an Illumina TruSeq RNA Sample Prep Kit (Illumina, San Diego, CA, USA) and sequenced as single-end reads on an Illumina NextSeq500 instrument. Short reads (< 30 bp) were removed from the Fastq files, as were reads with at least 95% of nucleotides with a low-quality score (quality score < 30) using fastp (Chen et al. 2018). All clean sequencing reads were mapped to the *O. sativa* reference genome (MSU Rice Genome Annotation Project Release 7) with STAR-2.7.3a (Dobin et al. 2013), and a read count table was created using featurecounts (Liao et al. 2014). Count tables were used for normalization and clustering analysis by iDEP.96 (Ge et al. 2018). GO enrichment analysis was performed on the ShinyGO 0.80 with default settings (Ge et al. 2020). Differentially expressed genes were identified with DESeq2 (Love et al. 2014) with the false discovery rate (FDR) < 0.05 and absolute $\log_2$-transformed fold-change ≥ 1. Boxplots representing the transcripts per million (TPM) values were plotted using R (v3.3.2 or later version).

Quantification of Phytohormone Contents

Samples were collected with a razor blade and consisted of 1-cm segments including an axillary bud, one node, and an internode (from 3 mm below to 7 mm above the node) from the shoot apical meristem part of the aerial shoot and the rhizome. Aerial shoot samples were collected from IRGC110404 at 5-leaf stage (vegetative stage), from Nipponbare at 5-leaf stage (vegetative stage), and from Nipponbare after induction of the inflorescence meristem around 12-leaf stage (reproductive stage). Based on bud morphology, samples were collected from the tip and the middle part of mature rhizomes (5 cm < length < 10 cm) where the rhizome bud before and after bending are respectively located. In addition, short rhizomes (length < 5 cm) were collected. Samples were collected from eight individuals or from four individuals for the reproductive aerial shoot of Nipponbare. The excised samples were washed three times with deionized water, flash-frozen in liquid nitrogen, and freeze-dried under vacuum (LABCONCO, Kansas). Freeze-dried tissues were crushed to a fine powder using a TissueLyser (Qiagen, Hilden, Germany) with a zirconia bead (diameter, 5 mm) in a 2-mL microcentrifuge tube. Phytohormone extraction and fractionation for phytohormone detection were performed according to a previously described method (Kojima et al. 2009; Kojima and Sakakibara 2012). The contents of cytokinins were measured using ultra-performance liquid chromatography (UPLC) and ODS columns (AQUITY UPLC HSS T3, 1.8 mm, 2.1 × 100 mm; Waters) combined with a tandem quadrupole mass spectrometer (qMS/MS) equipped with an electrospray interface (ESI; UPLC-ESI-qMS/MS, UPLC-Xevo TQ-S; Waters). Auxins, gibberellic acid (GA), abscisic acid (ABA), salicylic acid (SA), and jasmonic acid (JA) contents were determined with ultra-high performance liquid chromatography (UHPLC) and ODS columns (AQUITY UPLC HSS T3, 1.8 mm, 2.1 × 100 mm; Waters) combined with a quadrupole-orbitrap mass spectrometer (UHPLC/Q-Exactive™; Thermo Scientific) equipped with an electrospray interface as described previously (Shinozaki et al. 2015).

Principal Component Analysis (PCA) of Phytohormone Contents

PCA was performed on phytohormone contents, including all precursors and final products for GA, auxin, cytokinins, ABA, JA, and SA. The analysis was performed using the correlation matrix of trait values with prcomp and the setting "scale = TRUE". PCA loadings were obtained from the eigenvectors of the correlation matrix used for PCA computation. Specifically, the loadings were extracted from the rotation matrix returned by the prcomp function. Each loading represents the correlation coefficient between a given principal component and the original trait variables. The prcomp function automatically normalizes the eigenvectors to unit length, ensuring that each principal component is a linear combination of standardized trait values.

In Situ hybridization of *OlGA20ox2* in Rhizome Buds

For synthesizing first strand cDNA, we used 1 µg of total RNA extracted from *O. longistaminata* as a template using the oligo-dT primer supplied with SuperScript™ IV kit (Thermo Scientific, USA). For generation of gene-specific probes, *OlGA20ox2* cDNA fragments were amplified using the gene-specific primers SD1_in_situ_EcoRV_F 5′-CCCTCGAGCTACTTCTCCAGCACCCTCG-3′, and SD1_in_situ_XhoI_R 5′-CTGATATCCCTGTGCAGGC AGCTCTTAT-3′ and ligated into the pBluescript II SK + vector. Rhizome buds of *O. longistaminata* were fixed in 4% (w/v) paraformaldehyde and 0.25% (v/v) glutaraldehyde in 0.1 M sodium phosphate buffer (pH 7.2) overnight at 4 °C before being embedded in SCEM compound

(SECTION-LAB, Japan). The surface to be cut was covered with adhesive film (Cryofilm type IIC9, SECTION-LAB, Japan), and frozen Sects. (8–14 μm) were prepared with a cryostat (CM1850 Leica Microsystems, Germany) as previously described (Kawamoto 2003). Digoxygenin-labeled RNA probes were transcribed in vitro with T7 RNA polymerase (Roche, Basel). Hybridization and immunological detection of the hybridized probes were performed according to a published method (Kouchi and Hata 1993) with some modifications.

Alignment of the GA20ox2 Amino Acid Sequence

The *O. longistaminata* GA20ox2 (OlGA20ox2) protein sequence was retrieved from the *O. longistaminata* information resource (http://olinfres.nig.ac.jp) using OL01G003890 as gene ID (Table S4). The *O. sativa* japonica cv. Nipponbare GA20ox2 (OsGA20ox2) protein sequence was retrieved from RAP-DB (https://rapdb.dna.affrc.go.jp/) using the gene ID Os01 g0883800, and the deepwater rice (cv. C9285) GA20ox2 (OsGA20ox2_C9) protein sequence was retrieved from a previous work (Kuroha et al. 2018). Protein sequences were aligned using the ClustalW program. The number of amino acid substitutions between each pair of GA20ox2 orthologs was estimated using the Jones–Taylor–Thornton (JTT) model with a complete deletion option.

Gibberellin and Uniconazole Treatments of Cuttings

Plants carrying new rhizome buds on the third node of the primary tiller at the 5-leaf stage were used for phytohormone treatments, which were carried out in soil (Mikawa-baido, Aichi). Various concentrations of GA_4 (10^{-7}, 10^{-6}, and 10^{-5} M) together with the GA biosynthesis inhibitor uniconazole (UNI; 10^{-5} M, WAKO, Osaka) or mock solvent (0.1% [v/v] ethanol) were added to the water at the beginning of the treatments. Three individuals were used for each treatment. The entire setup was placed in a controlled environment chamber (LP-2P; Nippon Ikakikai Seisakujo, Osaka) set to a 14-h light/10-h dark photoperiod, average humidity of 65.7%, and an average temperature of 30.4 °C.

Transcriptome Analysis Using Cuttings With or Without GA_4 and UNI Treatments

Detailed diagrams of the sampling strategy are shown in Fig. S7. We treated 10^{-5} M UNI alone or 10^{-5} M UNI + 10^{-7} M GA_4 to IRGC110404 (*O. longistaminata*) and T65 (*O. sativa*) cuttings at the 4-leaf stage. Then, second axillary buds on the third node at the 5-leaf stage of cuttings were collected after each treatment. All the axillary bud sampled had not bent at the sampling point. Control samples were mock-treated with solvent only (0.1% [v/v] ethanol). Three axillary buds located on the third node of cuttings were collected in one tube and used as one replicate. Three replicates were prepared for each sample (control, UNI treatment, UNI + GA_4 treatment). Total RNA was extracted from the collected samples using RNeasy Plant Kit (QIAGEN) following the manufacturer's instructions. Sequencing libraries were constructed using a TruSeq RNA Sample Prep Kit (Illumina) and sequenced as paired-end reads on an Illumina HiSeq 2000 instrument. All sequencing reads were mapped to the *O. sativa* reference genome (MSU Rice Genome Annotation Project Release 7) with STAR-2.7.3a (Dobin et al. 2013). The R package edgeR was used to normalize gene counts to counts per million (cpm) values (Robinson et al. 2010). GO term enrichment analysis was performed using the GOseq package in R as described previously (Nozue et al. 2015), using a *P*-value of 0.05 as threshold for statistically significant enrichment.

Quantification and Statistical Analysis

One-way analysis of variance (ANOVA) with a multi-comparison Tukey's honestly significant difference (HSD) *post hoc* test or a Student's *t*-test was used to evaluate statistical significance between groups. Experimental sample sizes and details of statistical methods are given in the figure legends.

Supplementary Information

The online version contains supplementary material available at https://doi.org/10.1186/s12284-025-00798-0.

Supplementary file1

Supplementary file2

Acknowledgements

We thank Ms. Joie Ramos and Dr. Kshirod K. Jena (International Rice Research Institute, IRRI) for sharing plant materials for the ***Oryza longistaminata*** accession, IRGC110404. We appreciate Dr. Shinjiro Yamaguchi (Kyoto University) for providing synthetic GA_4 for physiological assays. We deeply thank the National Bio-Resource Project (NBRP).

Author Contributions

KBU, MA, and TH designed this study and wrote the manuscript. KBU and TH grew samples and prepared sections. KBU and TO prepared the samples for phytohormone quantification. MK, YT, and HS performed phytohormone quantifications by LC–MS/MS. KN and AA helped with the cutting experiments. TH conducted GA and UNI treatments. KBU, TS, SR and TH performed RNA-seq analysis. All authors reviewed and commented on the manuscript.

Funding

This work was supported by the Core Research for Evolutional Science and Technology (grant no. JPMJCR13B1 to MA) by the Japan Science and Technology Agency (JST) and by JSPS KAKENHI (grant no. 20H05912 and 22H04978 to MA).

Data Availability

All datasets supporting the results and conclusions of this manuscript are included in the article and supplementary files. Materials generated in this study are maintained at Nagoya University, Japan. All sequencing reads generated for RNA-seq (PRJDB18052 and PRJDB20201) have been uploaded to the DNA Databank of Japan (DDBJ) repository.

Declarations

Ethics Approval and Consent to Participate
Not applicable.

Consent for Publication
Not applicable.

Competing Interests
The authors declare no competing interests.

Received: 2 April 2025 / Accepted: 13 May 2025
Published online: 24 May 2025

References

Bergonzi S, Albani MC, van Loren EV et al (2013) Mechanisms of age-dependent response to winter temperature in perennial flowering of *Arabis alpina*. Science 340:1094–1097. https://doi.org/10.1126/science.1234116
Bessho-Uehara K, Nugroho JE, Kondo H et al (2018) Sucrose affects the developmental transition of rhizomes in *Oryza longistaminata*. J Plant Res 131:693–707. https://doi.org/10.1007/s10265-018-1033-x
Bowman JL (1997) Evolutionary conservation of angiosperm flower development at the molecular and genetic levels. J Biosci 22:515–527. https://doi.org/10.1007/BF02703197
Caruana JC, Sittmann JW, Wang W, Liu Z (2018) Suppressor of runnerless encodes a DELLA protein that controls runner formation for asexual reproduction in strawberry. Mol Plant 11:230–233. https://doi.org/10.1016/j.molp.2017.11.001
Chanderbali AS, Yoo M-J, Zahn LM et al (2010) Conservation and canalization of gene expression during angiosperm diversification accompany the origin and evolution of the flower. Proc Natl Acad Sci 107:22570–22575. https://doi.org/10.1073/pnas.1013395108
Chen S, Zhou Y, Chen Y, Gu J (2018) FASTP: an ultra-fast all-in-one FASTQ preprocessor. Bioinformatics 34:i884–i890. https://doi.org/10.1093/bioinformatics/bty560
Cronquist A (1968) The evolution and classification of flowering plants. Thomas Nelson & Sons Ltd
Devlin PF, Kay SA (2000) Flower arranging in *Arabidopsis*. Science 288:1600–1602. https://doi.org/10.1126/science.288.5471.1600
Dobin A, Davis CA, Schlesinger F et al (2013) STAR: ultrafast universal RNA-seq aligner. Bioinformatics 29:15–21. https://doi.org/10.1093/bioinformatics/bts635
Fan Z, Cai Z, Shan J, Yang J (2017) Letter to the editor: bud position and carbohydrate play a more significant role than light condition in the developmental transition between rhizome buds and aerial shoot buds of *Oryza longistaminata*. Plant Cell Physiol 58:1281–1282. https://doi.org/10.1093/pcp/pcx061
Ge SX, Son EW, Yao R (2018) iDEP: an integrated web application for differential expression and pathway analysis of RNA-Seq data. BMC Bioinform 19:534. https://doi.org/10.1186/s12859-018-2486-6
Ge SX, Jung D, Yao R (2020) ShinyGO: a graphical gene-set enrichment tool for animals and plants. Bioinformatics 36:2628–2629. https://doi.org/10.1093/bioinformatics/btz931
Hannapel DJ, Sharma P, Lin T, Banerjee AK (2017) The multiple signals that control tuber formation. Plant Physiol 174:845–856. https://doi.org/10.1104/pp.17.00272
He R, Kim M-J, Nelson W et al (2012) Next-generation sequencing-based transcriptomic and proteomic analysis of the common reed, *Phragmites australis* (Poaceae), reveals genes involved in invasiveness and rhizome specificity. Am J Bot 99:232–247. https://doi.org/10.3732/ajb.1100429
He R, Salvato F, Park J-J et al (2014) A systems-wide comparison of red rice (*Oryza longistaminata*) tissues identifies rhizome specific genes and proteins that are targets for cultivated rice improvement. BMC Plant Biol 14:46. https://doi.org/10.1186/1471-2229-14-46
Hu F, Wang D, Zhao X et al (2011) Identification of rhizome-specific genes by genome-wide differential expression analysis in *Oryza longistaminata*. BMC Plant Biol 11:18. https://doi.org/10.1186/1471-2229-11-18
Jang CS, Kamps TL, Skinner DN et al (2006) Functional classification, genomic organization, putatively cis-acting regulatory elements, and relationship to quantitative trait loci, of sorghum genes with rhizome-enriched expression. Plant Physiol 142:1148–1159. https://doi.org/10.1104/pp.106.082891
Kaneko-Suzuki M, Kurihara-Ishikawa R, Okushita-Terakawa C et al (2018) TFL1-like proteins in rice antagonize rice FT-like protein in inflorescence development by competition for complex formation with 14-3-3 and FD. Plant Cell Physiol 59:458–468. https://doi.org/10.1093/pcp/pcy021
Kawai M, Tabata R, Ohashi M et al (2022) Regulation of ammonium acquisition and use in *Oryza longistaminata* Ramets under nitrogen source heterogeneity. Plant Physiol. https://doi.org/10.1093/plphys/kiac025
Kawamoto T (2003) Use of a new adhesive film for the preparation of multi-purpose fresh-frozen sections from hard tissues, whole-animals, insects and plants. Arch Histol Cytol 66:123–143. https://doi.org/10.1679/aohc.66.123
Kepinski S (2006) Integrating hormone signaling and patterning mechanisms in plant development. Curr Opin Plant Biol 9:28–34. https://doi.org/10.1016/j.pbi.2005.11.001
Klimes L, Klimesova J, Hendriks R, Groenendael JV (1997) Clonal plant architecture: a comparative analysis of form and function. In: In the ecology and evolution of clonal plants. Backhuys, pp 1–29. ISBN: 978-90-73348-73-8.
Kloosterman B, Navarro C, Bijsterbosch G et al (2007) StGA2ox1 is induced prior to stolon swelling and controls GA levels during potato tuber development: role for a GA 2-oxidase in potato tuber development. Plant J 52:362–373. https://doi.org/10.1111/j.1365-313X.2007.03245.x
Kojima M, Sakakibara H (2012) Highly sensitive high-throughput profiling of six phytohormones using MS-probe modification and liquid chromatography–tandem mass spectrometry. In: Normanly J (ed) High-throughput phenotyping in plants. Humana, Totowa, NJ, pp 151–164
Kojima M, Kamada-Nobusada T, Komatsu H et al (2009) Highly sensitive and high-throughput analysis of plant hormones using MS-probe modification and liquid chromatography–tandem mass spectrometry: an application for hormone profiling in *Oryza sativa*. Plant Cell Physiol 50:1201–1214. https://doi.org/10.1093/pcp/pcp057
Kouchi H, Hata S (1993) Isolation and characterization of novel nodulin cDNAs representing genes expressed at early stages of soybean nodule development. Mol Gen Genet 238–238:106–119. https://doi.org/10.1007/BF00279537
Kuijt SJH, Greco R, Agalou A et al (2014) Interaction between the *GROWTH-REGULATING FACTOR* and *KNOTTED1-LIKE HOMEOBOX* families of transcription factors [W]. Plant Physiol 164:1952–1966. https://doi.org/10.1104/pp.113.222836
Kuroha T, Nagai K, Gamuyao R et al (2018) Ethylene-gibberellin signaling underlies adaptation of rice to periodic flooding. Science 361:181–186. https://doi.org/10.1126/science.aat1577
Lian X, Zhong L, Bai Y et al (2024) Spatiotemporal transcriptomic atlas of rhizome formation in *Oryza longistaminata*. Plant Biotechnol J 22:1652–1668. https://doi.org/10.1111/pbi.14294
Liao Y, Smyth GK, Shi W (2014) featureCounts: an efficient general purpose program for assigning sequence reads to genomic features. Bioinformatics 30:923–930. https://doi.org/10.1093/bioinformatics/btt656
Love MI, Huber W, Anders S (2014) Moderated estimation of fold change and dispersion for RNA-seq data with DESeq2. Genome Biol 15:550. https://doi.org/10.1186/s13059-014-0550-8
Navarro C, Abelenda JA, Cruz-Oró E et al (2011) Control of flowering and storage organ formation in potato by FLOWERING LOCUS T. Nature 478:119–122. https://doi.org/10.1038/nature10431
Nozue K, Tat AV, Kumar Devisetty U et al (2015) Shade avoidance components and pathways in adult plants revealed by phenotypic profiling. PLoS Genet 11:e1004953. https://doi.org/10.1371/journal.pgen.1004953
Robinson MD, McCarthy DJ, Smyth GK (2010) edgeR: a bioconductor package for differential expression analysis of digital gene expression data. Bioinformatics 26:139–140. https://doi.org/10.1093/bioinformatics/btp616
Romera-Branchat M, Andrés F, Coupland G (2014) Flowering responses to seasonal cues: what's new? Curr Opin Plant Biol 21:120–127. https://doi.org/10.1016/j.pbi.2014.07.006
Shibasaki K, Takebayashi A, Makita N et al (2021) Nitrogen nutrition promotes rhizome bud outgrowth via regulation of cytokinin biosynthesis genes and an *Oryza longistaminat*a ortholog of FINE CULM 1. Front Plant Sci 12:670101. https://doi.org/10.3389/fpls.2021.670101
Shinozaki Y, Hao S, Kojima M et al (2015) Ethylene suppresses tomato (*Solanum lycopersicum*) fruit set through modification of gibberellin metabolism. Plant J 83:237–251. https://doi.org/10.1111/tpj.12882
Simpson GG, Gendall AR, Dean C (1999) When to switch to flowering. Annu Rev Cell Dev Biol 15:519–550. https://doi.org/10.1146/annurev.cellbio.15.1.519
Taoka K, Ohki I, Tsuji H et al (2011) 14-3-3 proteins act as intracellular receptors for rice Hd3a florigen. Nature 476:332–335. https://doi.org/10.1038/nature10272

Tenreira T, Lange MJP, Lange T et al (2017) A specific gibberellin 20-oxidase dictates the flowering-runnering decision in diploid strawberry. Plant Cell 29:2168–2182. https://doi.org/10.1105/tpc.16.00949

Teotia S, Tang G (2015) To bloom or not to bloom: role of MicroRNAs in plant flowering. Mol Plant 8:359–377. https://doi.org/10.1016/j.molp.2014.12.018

Toriba T, Tokunaga H, Shiga T et al (2019) BLADE-ON-PETIOLE genes temporally and developmentally regulate the sheath to blade ratio of rice leaves. Nat Commun 10:619. https://doi.org/10.1038/s41467-019-08479-5

Toriba T, Tokunaga H, Nagasawa K et al (2020) Suppression of leaf blade development by BLADE-ON-PETIOLE orthologs is a common strategy for underground rhizome growth. Curr Biol 30:509–516e3. https://doi.org/10.1016/j.cub.2019.11.055

Turck F, Fornara F, Coupland G (2008) Regulation and identity of florigen: FLOWERING LOCUS T moves center stage. Annu Rev Plant Biol 59:573–594. https://doi.org/10.1146/annurev.arplant.59.032607.092755

Wang K, Li J, Fan Y, Yang J (2024) Temperature effect on rhizome development in perennial rice. Rice 17:32. https://doi.org/10.1186/s12284-024-00710-2

Yoshida A, Terada Y, Toriba T et al (2016) Analysis of rhizome development in *Oryza longistaminata*, a wild rice species. Plant Cell Physiol 57:2213–2220. https://doi.org/10.1093/pcp/pcw138

Zhang X, Campbell R, Ducreux LJM et al (2020) TERMINAL FLOWER-1/CENTRORADIALIS inhibits tuberisation via protein interaction with the tuberigen activation complex. Plant J 103:2263–2278. https://doi.org/10.1111/tpj.14898

Zheng R, Meng X, Hu Q et al (2023) OsFTL12, a member of FT -like family, modulates the heading date and plant architecture by florigen repression complex in rice. Plant Biotechnol J 21:1343–1360. https://doi.org/10.1111/pbi.14020

Zhou C-M, Zhang T-Q, Wang X et al (2013) Molecular basis of age-dependent vernalization in *Cardamine flexuosa*. Science 340:1097–1100. https://doi.org/10.1126/science.1234340

Publisher's Note